SAND2020-12428C

Estimation of PV Location based on Voltage Sensitivities in Distribution Systems with Discrete Voltage Regulation Equipment

Cristian Gómez-Peces, Santiago Grijalva
Georgia Institute of Technology

Matthew J. Reno, Logan Blakely
Sandia National Laboratory

***Abstract*— High penetration of solar photovoltaics can have a significant impact on the power flows and voltages in distribution systems. In order to support distribution grid planning, control and optimization, it is imperative for utilities to maintain an accurate database of the locations and sizes of PV systems. This paper extends previous work on methods to estimate the location of PV systems based on knowledge of the distribution network model and availability of voltage magnitude measurement streams. The proposed method leverages the expected impact of solar injection variations on the circuit voltage and takes into account the operation and impact of changes in voltage due to discrete voltage regulation equipment (VRE). The estimation model enables determining the most likely location of PV systems, as well as voltage regulator tap and switching capacitors state changes. The method has been tested for individual and multiple PV system, using the Chi-Square test as a metric to evaluate the goodness of fit. Simulations on the IEEE 13-bus and IEEE 123-bus distribution feeders demonstrate the ability of the method to provide consistent estimations of PV locations as well as VRE actions.**

***Index Terms*—Solar Photovoltaic, Distribution Circuit, Voltage Sensitivities, Location Estimation, Voltage Regulator, Switching Capacitor, VRE.**

I. Introduction

The integration of solar photovoltaics (PV) in distribution systems continues at a fast pace. The technological advances and economies of scale facilitate the rapid adoption of this energy source in both residential systems, and medium-size commercial and industrial customers. However, many utilities continuously face challenges such as over-voltages, unexpected back-feeding and other reliability problems due to the incorporation of new PV systems [1]. It is imperative for utilities to maintain an updated record of PV interconnections. In addition to these possible technical issues, solar generation needs to be taken into account for effective distribution grid planning [2], operation, and for maintaining a safe operation of control devices. In many cases, databases are not accurate, or some PV systems may have been connected to the grid without a permit. Utilities are interested in maintaining and validating their databases in order to prevent errors in terms of the PV location, the phase to which it is connected, the PV size, and the PV array orientation [3]. According to the utility survey conducted by EPRI [4], 63% of utilities do not record the PV tilt and azimuth and 74% do not have any metering on residential PV systems. In addition, database error checking such as phase identification can be a labor-intensive process. The proposed method predicts the most likely PV location based on PV injection estimations.

Several approaches have been proposed in the literature to determine the PV generation based on data-driven methods. The study in [5] uses an approach that exploits the high correlation of diurnal and nocturnal demands by using Gaussian mixture models and maximum likelihood estimation-based techniques to disaggregate customer-level behind-the-meter (BTM) PV generation. An unsupervised framework is presented in [6] for joint disaggregation of the net load readings into the solar PV generation and electric load, where estimations are made based on a mixed hidden Markov model (MHMM). Other studies use deep learning, as in [7], to estimate behind the meter (BTM) residential PV size, tilt and azimuth, reporting an upper-bound error of 3.98% and robustness even when using training data with incorrect tilt and azimuth values. However, the overall literature lacks methods that exploit the relation between voltage measurements and power injections and that consider voltage control devices [8].

The work presented in [8] achieves accurate estimations of the PV injections, but it does not support cases that includes the operation of VREs. The work in [2] presents a study of the PV injection, tap changes and switching capacitor impacts on the system voltages, and [9] also defines the impact in terms of sensitivity planes. These core-fundamental concepts are leveraged in this study to estimate active power injections, and VRE actions.

Various methods have been proposed to estimate the tap setting of voltage regulators. In [10], the authors introduce a slight modification into the power system state estimation to predict both the voltage turns ratio and the phase-shift angle of

This material is based upon work supported in part by the U.S. Department of Energy's Office of Energy Efficiency and Renewable Energy (EERE) under Solar Energy Technologies Office (SETO) Agreement Number 34226. Sandia National Laboratories is a multi-mission laboratory managed and operated by National Technology and Engineering Solutions of Sandia, LLC., a wholly owned subsidiary of Honeywell International, Inc., for the U.S. Department of Energy's National Nuclear Security Administration under contract DE-NA0003525.

C. Gómez-Peces and S. Grijalva are with the Georgia Institute of Technology, Atlanta, GA, 30332 (cpeces3@gatech.edu, sgrijalva6@gatech.edu).

M. J. Reno and L. Blakely are with Sandia National Laboratory, Albuquerque, NM, 87123 (e-mails: mjreno@sandia.gov, lblakel@sandia.gov)

transformers. The authors in [11] present a method to estimate the tap positions based on the residuals from the state estimation, incorporating prior measurement and tap position information to increase robustness when dealing with bad data. Despite this, there are no methods that use sensitivity analysis to estimate the tap changes given in a voltage measurement stream. This paper presents a novel combination of the PV and VRE sensitivity analysis models to predict both PV locations and VRE actions. The theoretical concepts, such as VRE sensitivities, will be reinforced by illustrations based on the results obtained for the IEEE 13-bus test feeder. The numerical results will be based on the IEEE 123-bus to show the method's functionality on a larger and more realistic test feeder.

The rest of this paper is organized as follows: Section II presents the basic method for PV location estimation, Section III and IV describes the impact of switching capacitors and voltage regulators, respectively, Section V extends the method integrating PV and VRE estimations, Section VI shows numerical results on the IEEE 123-bus feeder. Sections VII and VIII discuss the method limitations and conclusions.

II. PV Location Estimation

The work in [8] provides a framework for the estimation of PV injections assuming knowledge of the distribution circuit model and availability of node voltage magnitude measurement data streams. The voltage magnitude at a node in the circuit has a fairly linear relationship with power injections. The coefficients depend on the status of the voltage regulating equipment, such that:

$$V_i(t) = V_i^0 + \alpha \Delta P_D(t) + \beta \Delta P_V(t) \quad (1)$$

where $\Delta P_D(t)$ is the change in demand and $\Delta P_V(t)$ is the change in PV injection, for each node i in a set of N nodes. Let us consider a set of candidate PV locations $\mathscr{L} = \{1,\ldots,\ell,\ldots L\}$.e.g. a set of nodes where the engineer suspects PV may exist. A matrix $\boldsymbol{S}$ is formed with the sensitivities of voltage with respect to PV injections:

$$s_{i\ell} = \partial V_i / \partial P_\ell \quad (2)$$

Sensing provides time series voltage measurements $\boldsymbol{V}$ and a time series of voltage changes $\boldsymbol{d}_{nt} = \boldsymbol{V}_{n,t+1} - \boldsymbol{V}_{n,t}$. The location of the PV system is estimated by finding the projection of $\boldsymbol{d}$ into the $\boldsymbol{S}_{nL}$ matrix subspace:

$$\hat{\boldsymbol{x}} = (\boldsymbol{S}^T\boldsymbol{S})^{-1}\boldsymbol{S}^T\boldsymbol{d} \quad (3)$$

Where $\hat{\boldsymbol{x}}$ is called the estimation vector and provides the PV injection estimation for that point in time. Estimation is possible if the matrix $\boldsymbol{S}$ has full rank. This implies that the columns of the matrix are linearly independent and the number of measurements is larger than the candidate locations to preserve sufficient degrees of freedom. In order to assess the goodness of fit, the χ^2 test is used. The estimated voltage increment given $\hat{\boldsymbol{x}}$ will be $\hat{\boldsymbol{d}} = \boldsymbol{S}\hat{\boldsymbol{x}}$. The measurement residuals are computed with the standard assumption that the smart meter class is 0.5%. Since that is the maximum error allowed, we defined the standard deviation approximately as third of the class, $\sigma_i = 0.0015$. We have that:

$$\zeta(\hat{\boldsymbol{x}}) = [\boldsymbol{S}\hat{\boldsymbol{x}} - \mathrm{d}]^T \boldsymbol{\Omega}^{-1} [\boldsymbol{S}\hat{\boldsymbol{x}} - \mathrm{d}] \quad (3)$$

where $\boldsymbol{\Omega}^{-1}$ is a diagonal matrix with entries $1/\sigma_i$. Finally, the confidence level of the estimation is given by:

$$\Pr[\chi^2 \geq \zeta] = 1.0 - \Pr[\zeta, \beta] \quad (4)$$

where β represents the degrees of freedom, calculated as the difference between the number of nodes being monitored and the number of PV location candidates.

III. Impact of Switching Capacitors

When the voltage magnitude data stream includes the effect of capacitor switching, the change in voltage will not result in an accurate estimation because it is caused by the injection of reactive power, and this sensitivity vector is not included in the $\boldsymbol{S}$ matrix. Typical discrete changes in voltage due to a capacitor can be observed in Fig. 1. The objective is not only to detect when these discontinuities happen to prevent imprecise estimations, but to also try to achieve accurate PV location estimation at those time points.

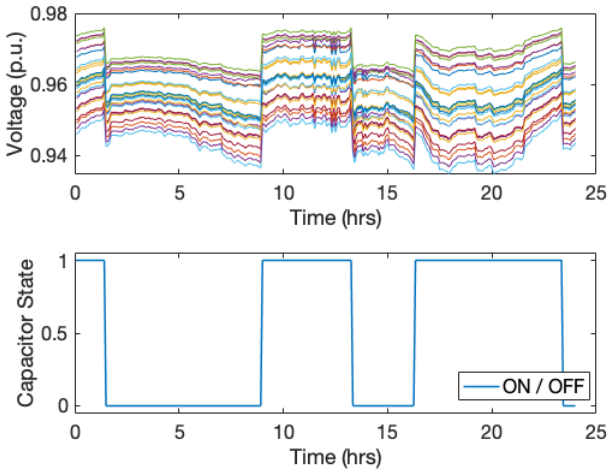

Fig. 1: Typical change in voltage due to a switching capacitor.

In order to incorporate the impact of capacitors switching in the method, one has to: a) estimate the impact on the active power sensitivities, b) compute the reactive power sensitivity and c) integrate the capacitor sensitivity as an additional column in the $\boldsymbol{S}$ matrix.

Let us consider the 3-phase switching capacitor at bus 680 in the IEEE 13-bus test feeder. When the capacitor is connected to grid, the inductance matrix of the power system changes. Therefore, all the sensitivities are expected to change. The impact of this change on the PV sensitivities was evaluated using an OpenDSS simulation. The capacitor was connected and disconnected in the simulation and active power sensitivities were calculated in each case. For a 500 kvar 3-phase capacitor, the PV sensitivity difference between states was under 2%, and the difference of most of sensitivity components was minimal. This means that the state of the existing switching capacitor has minimal impact on the active

power sensitivities of the distribution network, and the $\boldsymbol{S}$ matrix can be considered practically constant regardless of whether the capacitor status. However, when the capacitor switches between states, a discontinuity is introduced in the voltage stream. Fig. 2 describes the two sensitivity planes, which are largely parallel to each other. The increment of voltage due to a change in net demand will be contained in those planes. However, when the voltage steps out of the voltage control region, the capacitor changes its status resulting in a voltage increase – symbolized as a red vector that is not necessarily vertical – that is not contained in the sensitivity plane defined by $\boldsymbol{S}$. As result, the measurement vector cannot be expressed in terms of the sensitivity vectors and the estimation becomes inaccurate.

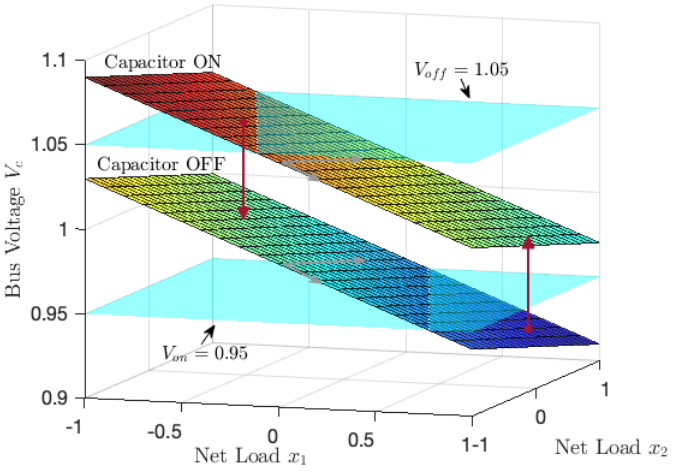

Fig. 2: Change of sensitivity planes due to capacitor state change.

Hence, our goal is to identify those points in time where the capacitor switches between states, while preserving the same sensitivity vectors that form the $\boldsymbol{S}$ matrix. In order to achieve this, a modification of the sensitivity matrix is introduced:

$$\boldsymbol{S} = [\boldsymbol{s_{PV}} \quad \boldsymbol{s_{Cap}}] \tag{5}$$

Here, s_{PV} corresponds to the set of columns of active power sensitivities that were already included, and s_{Cap} corresponds to the sensitivities associated with voltage changes in terms of reactive power injected by the capacitor. The sensitivities s_{Cap} can be computed by running 2 power flows: first with the capacitor disabled and then manually changing the state in OpenDSS, allowing us to compute the voltage difference due to the capacitor bank. As an example, Fig. 3 shows the voltage sensitivities for a 3-phase capacitor bank at bus 680. The larger the circles in the figure, the higher the sensitivity.

Since the size of the capacitor is known, these sensitivities can be adjusted in such way that the estimation will indicate the percentage of a capacitor state change:

$$s_{i,Cap} = \frac{\Delta V_i}{Q_{Cap}} \tag{6}$$

such that when a voltage increase due to capacitor occurs, the estimation components associated to capacitor actions shall be close to 100%.

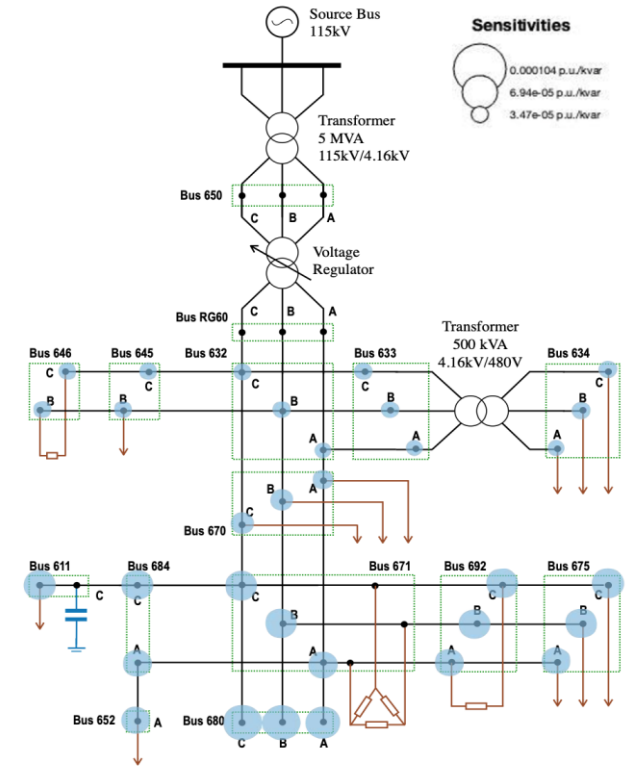

Fig. 3: Voltage increase due to the switching capacitor at bus 680 on the IEEE 13-bus test feeder.

IV. Impact of Voltage Regulators

Similarly, voltage regulators will cause a discontinuity in the voltage profile when the tap position changes, leading to a sensitivity hyperplane that practically has the same slope as that of the previous tap position.

In order to estimate both the tap change and the PV injection, a sensitivity associated to the voltage regulator action needs to be included in the $\boldsymbol{S}$ matrix. The VRE sensitivities are calculated by changing the taps on OpenDSS and subtracting the voltage recorded from both power flows. A tap change produces a homogenous increment in voltage of the same-phase node that comes after the regulator. Fig. 4 shows the voltage increments of a tap change for the bus 632A voltage regulator.

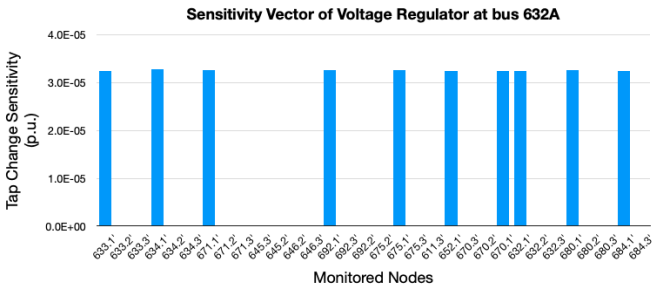

Fig. 4: Impact of voltage regulator at bus 632A in IEEE 13 feeder.

Once all VRE sensitivities have been determined, the modified $\boldsymbol{S}$ matrix is formed as:

$$\boldsymbol{S} = [\boldsymbol{s_{PV}} \quad \boldsymbol{s_{taps}}] \tag{7}$$

where the s_{taps} vector is calculated as:

$$s_{i,tap} = V_{i,tap+1} - V_{i,tap} \tag{8}$$

This increase is due to one tap change. If the tap changes two positions, the expected voltage increment will be double. Therefore, the method not only predicts when the voltage regulator takes action, but also the changed number of taps.

V. Integration of Voltage Regulation Equipment

The methodologies developed in sections III and IV are based on the use of a matrix of voltage sensitivities with respect to node power injections $\boldsymbol{S}$. However, in the presence of VRE, the impact of VRE actions and the PV power injection both may produce changes in voltage magnitude in the circuit nodes that result in sensitivity columns that are not linearly independent vectors. To illustrate this, let us consider Fig. 5, where a voltage change that is due to a VRE action can be expressed in terms of the PV sensitivity column vectors.

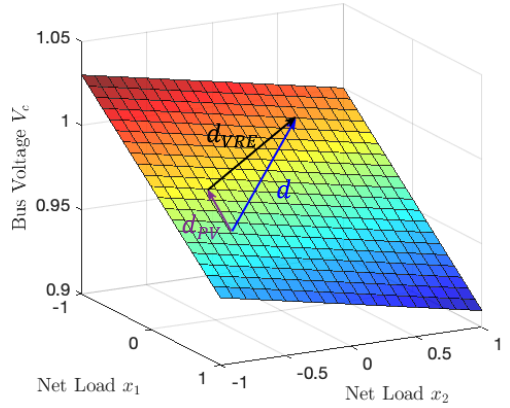

Fig. 5: VRE impact that is linearly dependent on PV sensitivities.

In such case, the Gramian of $\boldsymbol{S}$ becomes singular and $(\boldsymbol{S}^T\boldsymbol{S})^{-1}$ cannot be computed. Therefore, an approach must be developed that can estimate PV injections, tap changes, and switching capacitor actions regardless of the structure of $\boldsymbol{S}$.

The method extends the principles used for PV location and injection estimation by first determining whether a VRE actions is present in the voltage magnitude measurement data stream. Let us define $\hat{\boldsymbol{d}}_{VRE}$ as the estimation of the changes in voltage due to VRE actions in a distribution circuit. The correct estimation of the PV injections would discount the effect due to the VRE in changes in voltages $\boldsymbol{d}$:

$$\hat{\boldsymbol{x}} = (\boldsymbol{S}^T\boldsymbol{S})^{-1}\boldsymbol{S}^T(\boldsymbol{d} - \hat{\boldsymbol{d}}_{VRE}) \tag{9}$$

The changes in voltage occur in fixed amounts, proportional to the number of taps changed. It is possible to obtain an estimation of a voltage changes due to VRE, $\boldsymbol{d}_{VRE}$ by simulating VRE actions in the distribution circuit and performing an estimation for the resulting voltage changes. Let us denote the result of this estimation by $\hat{\boldsymbol{x}}_{VRE}$:

$$\hat{\boldsymbol{x}}_{VRE} = (\boldsymbol{S}^T\boldsymbol{S})^{-1}\boldsymbol{S}^T\boldsymbol{d}_{VRE} \tag{10}$$

This particular estimation vector corresponds to a single VRE device. A matrix $\boldsymbol{X}_{VRE}$ can be formed when considering all the VRE devices in the circuit:

$$\boldsymbol{X}_{VRE} = (\boldsymbol{S}^T\boldsymbol{S})^{-1}\boldsymbol{S}^T\boldsymbol{D}_{VRE} \tag{11}$$

where $\boldsymbol{X}_{VRE} = [\hat{\boldsymbol{x}}_{VRE_1}, \ldots, \hat{\boldsymbol{x}}_{VRE_K}]$, $\boldsymbol{D}_{VRE} = [\boldsymbol{d}_{VRE_1}, \ldots, \boldsymbol{d}_{VRE_K}]$ and K is the number of total VRE devices considered. We have that each vector $\hat{\boldsymbol{x}}_{VRE}$ in $\boldsymbol{X}_{VRE}$ is the expected footprint that a tap change will leave in the estimation. Once $\boldsymbol{X}_{VRE}$ has been determined, it can be used to determine the presence of tap change actions, if the resulting estimation vector is similar to $\hat{\boldsymbol{x}}_{VRE}$. When a change in voltage contains the impact of VRE and PV for a given point in time, the resulting estimation vector will contain components associated with both the PV location and the expected estimation $\hat{\boldsymbol{x}}_{VRE}$:

$$\boldsymbol{x}_{PV+VRE} = (\boldsymbol{S}^T\boldsymbol{S})^{-1}\boldsymbol{S}^T\boldsymbol{d} \tag{12}$$

The matrix $\boldsymbol{X}_{VRE}$ can now be used to determine whether any VRE action took place by performing a second estimation on the resulting estimation vector:

$$\boldsymbol{v} = ((\boldsymbol{X}_{VRE}^T\boldsymbol{X}_{VRE})^{-1}\boldsymbol{X}_{VRE}^T) \cdot \boldsymbol{x}_{PV+VRE} \tag{13}$$

The resulting vector v will provide non-zeros values for those components associated with the VRE devices that operated at that specific point in time. For example, if 2 step changes occurred for a certain voltage regulator, the resulting $\boldsymbol{v}$ component may be 2.03. For those devices that did not take action at that point in time, a value close to 0 will appear. A non-linear filter ϕ needs to be applied to remove the values close to zero and to obtain integer components from $\boldsymbol{v}$. For illustration purposes, let's consider the following example. Assume that there are 3 voltage regulators in a distribution circuit, and the results of our second estimation is: $\boldsymbol{v} = [0.04 \quad 0.98 \quad -0.01]^T$, then the filter $\phi(\boldsymbol{v}) = [0\ 1\ 0]^T$, which corresponds to the actual tap changes that occurred at that point in time. Once a VRE action is detected, the impact on the voltage is computed by multiplying by $\boldsymbol{X}_{VRE}$, which leads to the estimation components of tap change, and finally by $\boldsymbol{S}$, which leads to the estimated voltage increase due to that VRE action:

$$\hat{d}_{VRE} = \boldsymbol{S} \cdot \boldsymbol{X}_{VRE} \cdot \phi(\boldsymbol{v}) \tag{14}$$

With the subtraction of the impact of VRE on voltage increments it is not only possible to predict the location of PV systems, but also the action taken by controlling devices.

Putting together equations (11), (12), (13), and (14) in (9) the formulation of the method now becomes:

$$\hat{\boldsymbol{x}} = (\boldsymbol{S}^T\boldsymbol{S})^{-1}\boldsymbol{S}^T\Big(\boldsymbol{d} - \boldsymbol{S} \cdot \boldsymbol{X}_{VRE} \cdot \phi\big(((\boldsymbol{X}_{VRE}^T\boldsymbol{X}_{VRE})^{-1}\boldsymbol{X}_{VRE}^T)(\boldsymbol{S}^T\boldsymbol{S})^{-1}\boldsymbol{S}^T\boldsymbol{d}\big)\Big) \tag{15}$$

where:

- $\boldsymbol{S}$ is the sensitivity matrix. It has N rows and L columns.
- $\boldsymbol{d}$ is the measurement vector: $[\boldsymbol{d}_1, \ldots, \boldsymbol{d}_N]^T$.
- $\boldsymbol{X}_{VRE}$ includes all the estimation vectors due to VRE devices. It has L rows and K columns.

- $\boldsymbol{v}$ is the vector of estimated VRE actions. Hence its dimension is equal to the number of total VRE devices in the circuit: $[\boldsymbol{v}_1, \dots, \boldsymbol{v}_K]^T$.

N is the number of monitored nodes, L is the number of PV locations candidates, and K is the number of VRE devices considered. The number of tap changes can be predicted by looking at the term $\phi\big(((\boldsymbol{X}_{VRE}^T\boldsymbol{X}_{VRE})^{-1}\boldsymbol{X}_{VRE}^T)(\boldsymbol{S}^T\boldsymbol{S})^{-1}\boldsymbol{S}^T\boldsymbol{d}\big)$.

VI. Numerical Results

A. Case Description

The IEEE 123-bus distribution system operates at 4.16 kV and has an unbalanced loading. The circuit has a several voltage control devices in addition to the regulator located at the substation: a 1-phase regulator between nodes 9 and 14, two 1-phase regulators between 25 and 26, and three 1-phase voltage regulators between nodes 160 and 67. The system presents switches that have been configured to preserve a radial topology. It is assumed that voltage magnitude measurements are obtained from 10 IntelliRupters, which cover 8% of the per phase voltage magnitudes. The circuit topology and IntelliRupters location are presented in Fig. 6.

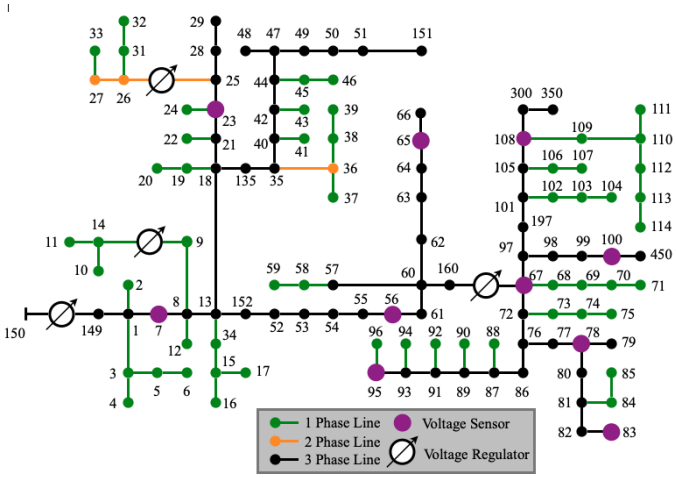

Fig. 6: Diagram of the IEEE 123-bus system.

To enable the algorithm to work with less available measurements, the number of PV location candidates must be lower to avoid singularities in the computations. In the results that follow below, different PV case scenarios are simulated to test the methodologies presented to address both linear dependent and independent impact of VRE. The PV profile is based on irradiance data provided by NREL [12] and represents the actual irradiation values observed on January 1, 2011 in Oahu, Hawaii. The time resolution selected for the QSTS simulations is 300 seconds.

B. Results with linearly independent VRE impact

The first experiment considered 9 different PV scenarios. Nine simulations were run placing a 1-phase 100 kW PV system at each of the nodes of buses 23, 197 and 83. In order to get an accurate estimation, it is necessary to look at points in time that are partly cloudy so that the node experiences large changes in PV injection. Based on the selected PV profile, the time window 12:25pm to 12:30pm is appropriate to estimate a PV injection. Fig. 7 shows the results of an estimation for this time frame in terms of two spider plots. The spider plots are graphical representations of the vectors $\hat{\boldsymbol{x}}$ and $\boldsymbol{v}$ for each simulation. The more a subplot in the spider plot tilts towards an outer label, the higher PV injection and hence a higher the probability of a PV system at that location. The more the plot bends closer to the inner zero points, the less likely it is that the PV is present at that location. Out of the 9 simulations, only the one with PV at node 23.1 experienced a tap change in voltage regulator 67A. As can be observed, the method is able to capture both the change in the PV injection (approximately 25 kW at that point in time) and the tap change.

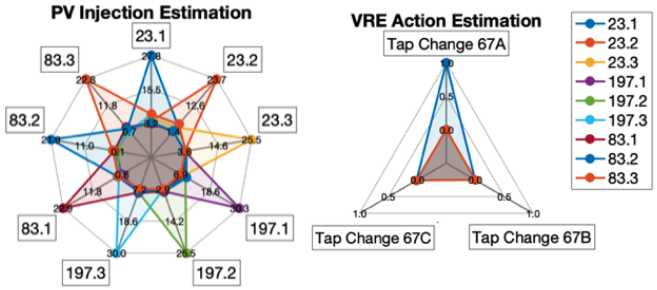

Fig. 7: PV and VRE Estimation results for simulations from 12:25pm to 12:30pm of 9 scenarios with a single PV.

The method works in the case of multiple PV as well, since for small PV injections the system behaves linearly. That is, the impact of 2 different PV systems on the voltage increment will be the sum of the resulting independent estimation. To verify this hypothesis, several simulations with multiple PV were run and analyzed. Fig. 8 shows the estimation results of three multiple PV case scenarios: 2 PVs at 21A and 56C, 2 PVs at 68A, 114A and 3 PVs at 7C, 105B and 97B for the time frame from 11:35am to 11:40am.

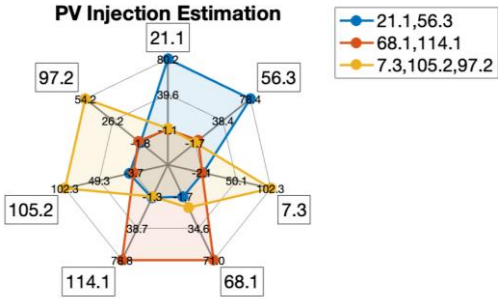

Fig. 8: PV estimation results for simulations from 12:25pm to 12:30pm of 3 scenarios with PV at multiple locations.

We observe that the method can detect and predict multiple PV injections with the same accuracy as with 1-phase PV. The Chi-Square test indicated a confidence level of 100% in all estimations.

C. Results with linearly dependent VRE impact

This section presents the particular case when the PV and VRE impacts are linearly dependent. This conflict causes singularities in the Gramian of $\boldsymbol{S}$ and hence it is necessary to use the formulation presented in (15). To represent this particular case, some buses close to bus 67 have been chosen as potential candidates. Let us consider buses 67, 62 and 68 as potential candidates. When $\boldsymbol{X}_{VRE}$ is calculated, it is verified that

the voltage regulator sensitivities can be expressed in terms of the sensitivity vectors associated to PV located at bus 62 and 67. Fig. 9 shows a bar chart of the vectors that compound $\boldsymbol{X}_{VRE}$. It can be observed that the impact of VRE affects the estimation at buses 67 and 62, but has little significant impact on bus 68. In addition, when $\widehat{\boldsymbol{D}}_{VRE} = \boldsymbol{S} \cdot \boldsymbol{X}_{VRE}$ is computed, we find that $\widehat{\boldsymbol{D}}_{VRE} = \boldsymbol{D}_{VRE}$ and the confidence level is equal to 1. This indicates that the VRE sensitivity falls within the PV sensitivity hyperplane.

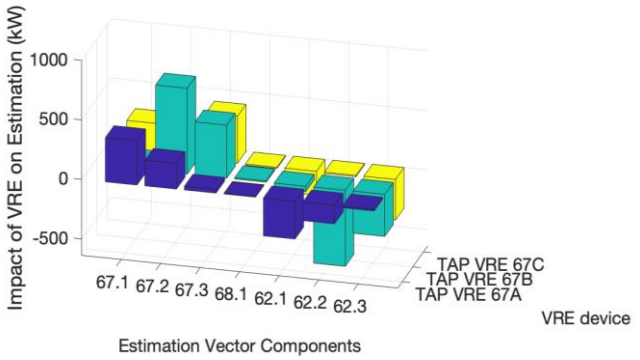

Fig. 9: Estimation of voltage increment due to VRE.

To test the accuracy of this methodology, several simulations were conducted placing PV systems at conflicting and non-conflicting nodes. These 7 simulations include a PV at each phase of buses 62, 67 and 68. The time window between 11:55am to 12:05pm had samples that included tap changes in addition to PV injection. Fig. 10 shows the resulting estimation. The method provides high accuracy predictions of the PV injection in addition to the exact 3 tap changes that occurred in the simulations with a PV located at 62B, 67A and 68A.

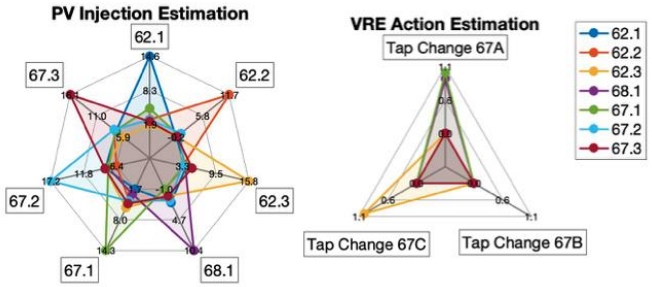

Fig. 10: PV and VRE Estimation for 7 simulations using (15).

VII. Limitations

The proposed method has the following limitations, which will require further analysis in a broader set of test cases:

a) It assumes a perfect model of the distribution feeder and no noise in the measurements. Real modes usually contain errors which will reduce the accuracy of the estimations.

b) When there is are multiple very high PV injections that cause a similar impact in the estimation as VREs ($\widehat{\boldsymbol{x}}_{VRE}$), the method may misclassify as a tap change. Very high PV injections are very unlikely due to hosting capacity limits.

c) The method takes as input the time-point voltage samples. However, some measurement devices only provide the average voltage over a sampling period, which leads to a measurement vector that can impact the accuracy of estimations.

VIII. Conclusions

A method has been described that is able to estimate PV locations with high accuracy, based on a limited number of available voltage magnitude measurement streams under the presence of voltage regulation equipment.

The impact of capacitors and voltage regulators on the estimation has been analyzed. The knowledge of the expected impact is used to determined when VRE actions took place. Depending on the structure of VRE is in terms of the PV sensitivities, two methodologies presented in this study can be utilized. If the increase of voltage is linearly independent from the expected voltage increment due to PV, VRE sensitivity can be added to the $\boldsymbol{S}$ matrix. On the other hand, if the impact is linearly dependent, a second estimation is required to determine the voltage increase due to VRE and to subtract it from the measurement vector. The simulations carried out on the IEEE 13-bus and IEEE 123-bus test feeders result in highly accurate results in terms of PV injection estimation, and VRE action detection.

References

[1] X. Zhang, S. Grijalva, "A Data-Driven Approach for Detection and Estimation of Residential PV Installations," IEEE Trans Smart Grid, 2016;7:2477–85.

[2] M.U. Qureshi, S. Grijalva, M.J. Reno, J. Deboever, X. Zhang and R.J. Broderick, "A Fast, Scalable Quasi-Static Time Series Analysis Method for PV Impact Studies using Linear Sensitivity Model", IEEE Transactions on Sustainable Energy, Vol 10, 2019.

[3] L. Blakely, M. J. Reno, and J. Peppanen, "Identifying Common Errors in Distribution System Models," IEEE Photovoltaic Specialists Conference (PVSC). 2019

[4] M. Hernandez, J. Peppanen, J. Deboever, M. Rylander, "Enhanced Load Modeling: Survey Results on Industry Load Modeling Practices"

[5] F. Bu, K. Dehgahnpour, Y. Yuan, Z. Wang, Y. Guo, "Disaggregating Customer-level Behind-the-Meter PV Generation Using Smart Meter Data", arXiv.org, Electrical Engineering and Systems Science, Signal Processing, arXiv:2009.00734.

[6] F. Kabir, N. Yu, W. Yao, R. Yang, Y. Zhang, "Joint Estimation of Behind-the-Meter Solar Generation in a Community,", 2020 IEEE Transactions on Sustainable Energy.

[7] K. Mason, M. J. Reno, S. Vejdan, S. Grijalva, "A Deep Neural Network Approach for Behind-the-meter Residential PV Size, Tilt and Azimuth Estimation", Solar Energy, 2020.

[8] S. Grijalva, A. U. Khan, J. S. Mbeleg, and C. Gomez-Peces, M. J. Reno, L. Blakely, "Estimation of PV Location in Distribution Systems based on Voltage Sensitivities", 2020 North American Power Symposium.

[9] M.U. Qureshi, S. Grijalva, M.J. Reno, "A Fast Quasi-Static Time Series Simulation Method for PV Smart Inverters with VAR Control using Linear Sensitivity Model", 7th World Conference on Photovoltaic Energy Conversion.

[10] M. Shiroie, S. H. Hosseini, "Observability and Estimation of Transformer Tap Setting with Minimal PMU Placement", 2008 IEEE Power and Energy Society General Meeting.

[11] E. Handschin, E. Kliokys "Transformer Tap Position Estimation and Bad Data Detection using Dynamic Signal Modelling," 1995 Transactions on Power Systems, Vol 10, No. 2, May 1995.

[12] Sengupta, Manajit; Andreas, Afshin (2014): Oahu Solar Measurement Grid (1-Year Archive): 1-Second Solar Irradiance; Oahu, Hawaii (Data). National Renewable Energy Laboratory. https://data.nrel.gov/submissions/11.